

Enhancement of Significant Wave Height Prediction through Aliasing Mitigation in Wave Radar Analysis

Jaehak Lee^a, Heesuk Yang^a, and Yonghwan Kim^{a,*}

^aDepartment of Naval Architecture and Ocean Engineering, Seoul National University, Seoul, Korea

Email: yhwankim@snu.ac.kr

1 Introduction

Attributed to its capability for remotely sensing a broad range of spatial-temporal sea surface information, the analysis of marine radar measurement data has emerged as an effective strategy for estimating sea state information. Nevertheless, because of constraints in temporal resolution, aliasing phenomena occur in fast Fourier transform (FFT)-based analysis, presenting a particularly critical challenge for ship-borne radar measurement systems. In this study, an enhanced procedure for estimating significant wave height is proposed by employing an aliasing mitigation strategy in analysis of marine radar image data.

2 Theoretical Backgrounds

In this study, the prediction of significant wave height is achieved by analyzing spatiotemporal marine radar image sequences through the concurrent implementation of two distinct procedures: statistical analysis of shadowing phenomena [1] and 3D-FFT-based spectral analysis [2].

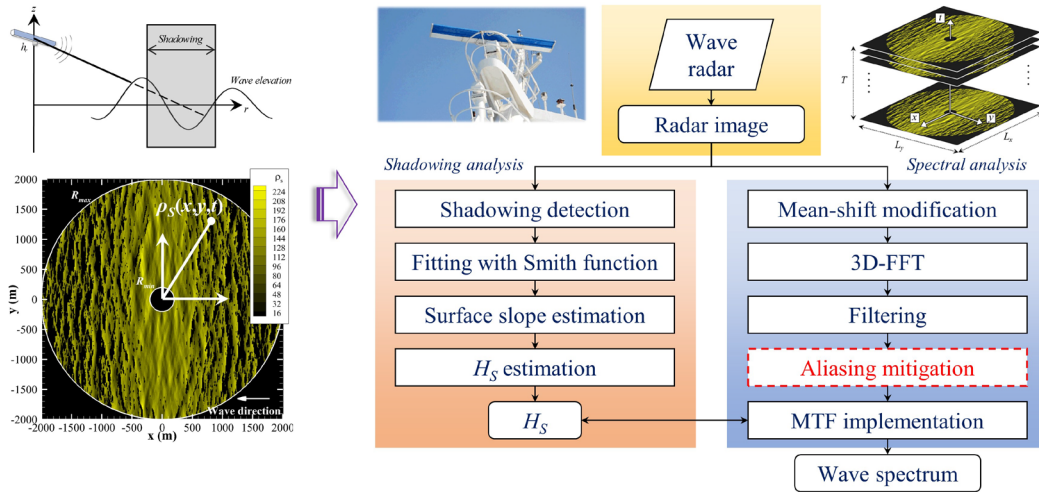


Figure 1: Comprehensive methodology for predicting significant wave height through marine radar image

In the spectral analysis, consecutive applications of mean shift modification, 3D-FFT, filtering (F), and modulation transfer function (MTF) are performed to retrieve a physically meaningful directional wave spectrum (S_{3D}) from raw radar image data (ρ_s). These procedures can be briefly summarized as follows:

$$\rho_m(x, y, t) = \begin{cases} \rho_s(x, y, t) - \beta_{mean} \times \text{mean}[\rho_s(x, y, t)] & \text{non-shadowing} \\ \rho_s(x, y, t) & \text{shadowing} \end{cases} \quad (1)$$

$$S_I(k_{x,j}, k_{y,k}, \omega_m) = \frac{1}{2dk_x dk_y d\omega} |A_{jkm}|^2, \quad \text{where } \rho_m(x, y, t) = \sum_{j,k,m} A_{jkm} e^{i(k_{x,j}x + k_{y,k}y - \omega_m t + \epsilon)} \quad (2)$$

$$S_{3D}(k_x, k_y, \omega) = MTF(F(S_I); \alpha_{MTF}, \beta_{MTF}) \quad (3)$$

where β_{mean} and $(\alpha_{MTF}, \beta_{MTF})$ indicate empirical parameters for the mean shift modification and MTF implementation, respectively, and S_{3D} denotes the wave spectrum defined in 3D wavenumber-frequency space (k_x, k_y, ω) [2]. The filtering and MTF procedures are utilized to alleviate the modulation effects attributed to the marine radar measurement mechanisms. Nevertheless, unphysical spectral energy is

still observed due to the aliasing of modulated high-frequency wave components, leading to a degradation in estimation accuracy [3]. Therefore, an additional aliasing mitigation procedure is required.

Firstly, the aliasing intersection region, defined as the overlap between the dispersion shell and unphysical aliased spectral energy, can be analytically determined in the 3D spectral domain (k_x, k_y, ω) using high-order dispersion relations and the symmetry of spectral energy.

$$\omega^{(p)} = \pm(1+p)\sqrt{\frac{g|\vec{k}|}{(1+p)}} + \vec{k} \cdot \vec{u} \quad \text{where } \vec{k} = (k_x, k_y), \vec{u} = (u_x, u_y) \quad (4)$$

$$S_{3D}(k_x, k_y, \omega) = S_{3D}(-k_x, -k_y, -\omega) \quad \text{and} \quad S_{3D}(k_x, k_y, \omega) = S_{3D}(k_x, k_y, \omega + 2m\omega_{Ny}) \quad (5)$$

Here, p represents the order of dispersion relations ($p=0, 1, 2, \dots$), and (u_x, u_y) is defined as the relative speed vector of surface current for radar machinery (ship, etc.). Attributed to the temporal under-sampling of measured radar image sequence, the Nyquist limit of wave frequency (ω_{Ny}) occurs in FFT applications and the wave energy $S_{3D}(k_x, k_y, \omega)$ is aliased in the 3D spectral domain. When $p=0$, Eq. (4) indicates dispersion shell region, employed for extracting meaningful wave energy components.

$$\omega = \pm\sqrt{g|\vec{k}| + |\vec{k}||\vec{u}|} \cos \gamma \quad \text{where } \cos \gamma = \frac{\vec{k} \cdot \vec{u}}{|\vec{k}||\vec{u}|} \quad (6)$$

The aliasing region of spectral energy, encompassing modulated wave components ($p>1$), can also be identified using symmetry and Nyquist periodicity of energy spectrum, as Eq. (5).

$$2m\omega_{Ny} \mp \omega = (1+p)\sqrt{\frac{g|\vec{k}|}{(1+p)}} \mp |\vec{k}||\vec{u}| \cos \gamma \quad (7)$$

The order of aliasing (m) is an arbitrary integer number, typically ranging between -2 and +2, contingent upon the magnitude of the relative surface current. The aliasing intersection region is finally determined from Eqs. (6) and (7) as follows:

$$|\vec{k}| = \frac{(2m\omega_{Ny})^2}{g(\sqrt{(1+p)+1})^2} \quad \text{and} \quad \omega = \pm \frac{2m\omega_{Ny}}{(\sqrt{(1+p)+1})} + \frac{(2m\omega_{Ny})^2}{g(\sqrt{(1+p)+1})^2} |\vec{u}| \cos \gamma \quad (8)$$

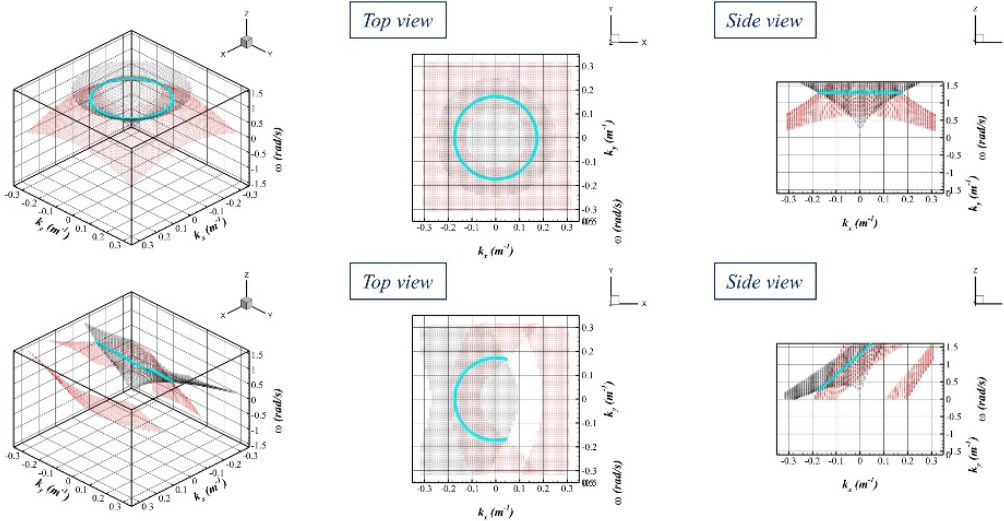


Figure 2: Illustration of identified aliasing intersection regions: $u_x=0.0\text{m/s}$ (top) and $u_x=6.0\text{m/s}$ (bottom).

Figure 2 illustrates examples of detected aliasing intersection regions in the 3D spectral domain. In these figures, the black-dotted region indicates the dispersion shell ($p=0$), while the red-dotted region reveals the aliasing of modulated spectral energy ($p=1$). The detected aliasing intersection regions for various p -values reveal concentric circles and are inclined in the direction of the surface current vector

within the 3D spectral domain. Then, a filtering procedure is introduced to alleviate the identified aliasing energy.

$$S_{3D}(k_x, k_y, \omega) = 0$$

$$\text{where } \begin{cases} \sqrt{k_x^2 + k_y^2} \geq k_m, \\ \tan^{-1}\left(\frac{k_y}{k_x}\right) \in [\pm\chi_{spr}^{(-)} + \pi, \pm\chi_{spr}^{(+)} + \pi], \end{cases} \quad k_m = \left[\frac{(2m\omega_{Ny})^2}{g(\sqrt{(1+p)+1})^2} \right]_{\min} = \frac{4}{9g} \omega_{Ny}^2 \Big|_{m=1, p=3} \quad (9)$$

$$S_{1D}(\chi_{spr}^{(-)}) = S_{1D}(\chi_{spr}^{(+)}) = \kappa S_{1D, \max}$$

Here, κ (with a specified value of 0.1) serves as the threshold for establishing the energy level criterion of the effective spreading angle, and S_{1D} represents a 1D wave spectrum defined regarding the incident wave heading. The wavenumber criterion (k_m) is established as the minimum radius within concentric circles of the identified aliasing intersection regions. From the obtained wave energy spectrum with aliasing mitigation, the high-order spectral moments are calculated as follows:

$$m_j = \int_0^{\omega_{Ny}} \int_{-k_{y,Ny}}^{k_{y,Ny}} \int_{-k_{x,Ny}}^{k_{x,Ny}} \omega^j S_{3D}(k_x, k_y, \omega) dk_x dk_y d\omega \quad (10)$$

In shadowing analysis, the surface slope (w_{est}) of the observed sea state is obtained using shadowing detection [4] and Smith's fitting with the shadowing probability density function [5]. Applying the shadowing detection algorithm to consecutive radar images allows the acquisition of the illumination ratio, signifying the probability of no shadowing occurrence. The obtained illumination ratio is then employed to fit the Smith function, facilitating the calculation of the surface slope (w_{est}).

Finally, significant wave height (H_S) can be determined as follows:

$$w_{total} = \sqrt{w_{est}(\theta)^2 + w_{est}\left(\theta + \frac{\pi}{2}\right)^2}, \quad T_4 = 2\pi \left(\frac{m_0}{m_4}\right)^{1/4} \quad (11)$$

$$H_S = \frac{g w_{total} T_4^2}{\pi^2} \quad (12)$$

3 Numerical Results

To validate the effectiveness of the proposed aliasing mitigation procedure, simulation-based synthetic radar image sequences were generated for various short-crested irregular sea conditions (H_S 1.0~6.0m). Considering the dependence of aliasing intersection regions on the relative speed of the surface current, radar images were generated for several ship speeds.

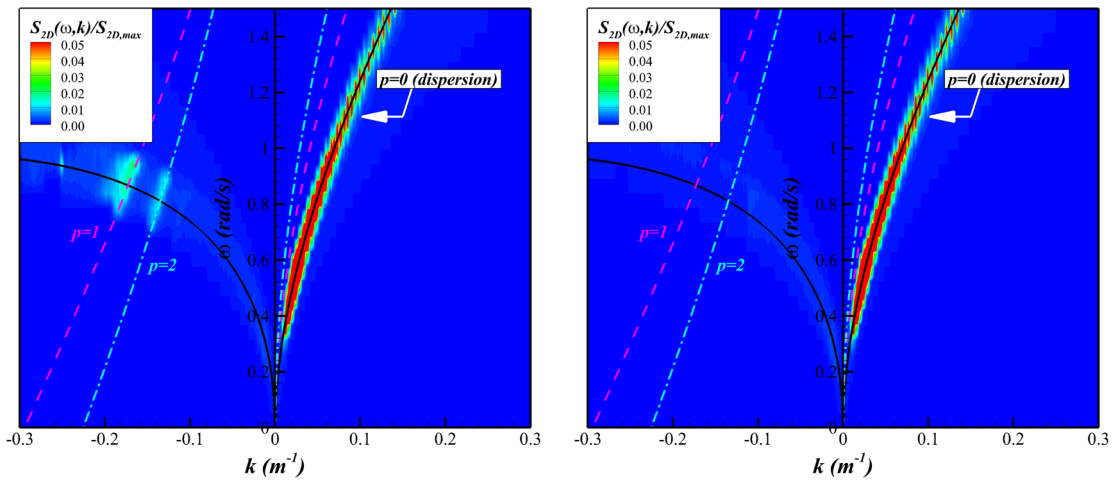


Figure 3: Examples of 2D (k, ω) spectrum without (left) and with (right) aliasing mitigation

The two-dimensional wavenumber-frequency spectrum (k, ω) was acquired and compared using 3D-FFT-based spectral analysis, as shown in Figure 3. In the absence of the aliasing mitigation procedure, unphysical energy distributions manifest in spectral regions opposite to the actual wave spectrum. These energy distributions correspond to the intersection regions between the dispersion shell ($p=0$ in Eq. (4))

and the aliasing energy of modulated high-order dispersion relation components ($p=1$ and 2 in Eq. (4)). It has been demonstrated that the proposed aliasing mitigation procedure effectively mitigated the unintended spectral energy arising from aliasing phenomena.

Utilizing the proposed procedure for aliasing mitigation, high-order spectral moments were calculated and the significant wave height was derived. In Figure 4, the prediction results of significant wave height are depicted for various ship speeds. It is evident that the estimation accuracy of significant wave height improved with the implementation of the aliasing mitigation procedure, particularly in severe sea states. This enhancement was primarily attributed to the reduction of high-frequency spectral energy arising from aliasing phenomena.

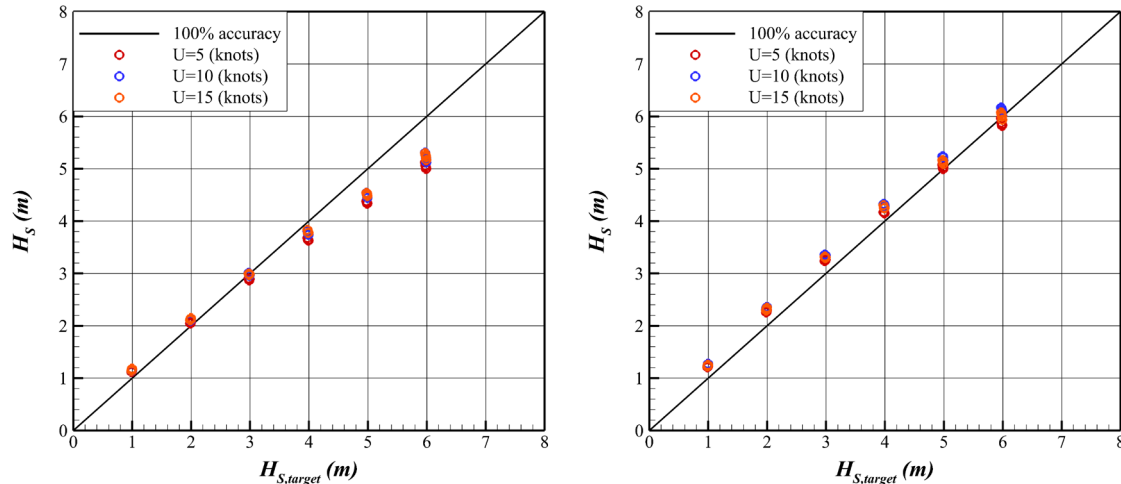


Figure 4: Prediction results of H_s for various ship speeds: without (left) and with (right) aliasing mitigation

4 Conclusions

The following conclusions are obtained from the present study

- The introduced aliasing mitigation procedure has proven to be effective in alleviating the unphysical energy distributions stemming from aliasing of modulated wave components in FFT analysis.
- The removal of these unphysical high-frequency energy components has contributed to the mitigation of underestimation in significant wave height prediction.

Acknowledgement

This work was supported by the Shipbuilding & Marine Industry Technology Development Program (20024292, Development of Digital Twin System for Health Management of Hull based on Marine Environment and Hull Response Measurement Data) funded by the Ministry of Trade, Industry & Energy (MOTIE, Korea).

References

- [1] Nam, Y. S. (2023). Study on real-time ocean wave analysis based on X-band radar measurement data. Master's thesis, Seoul National University.
- [2] Nieto-Borge, J. C. N., Rodriguez, G. R., Hessner, K. and Gonzalez, P. I. (2004). Inversion of marine radar images for surface wave analysis. *Journal of Atmospheric and Oceanic Technology*, 21(8), 1291-1300.
- [3] Seemann, J. and Ziemer, F. (1995). Computer simulation of imaging ocean wave fields with a marine radar. *Proceedings of OCEANS'95 MTS/IEEE*, 2, 1128-1133.
- [4] Gangeskar, R. (2014). An algorithm for estimation of wave height from shadowing in X-band radar sea surface images, *IEEE transactions on geoscience and remote sensing*, 52(6), 3373-3381.
- [5] Smith, B. (1967). Geometric shadowing of a random rough surface, *IEEE transaction on antennas and propagation*, 15, 668-671.